IET Generation, Transmission & Distribution

Special Issue: Interfacing Techniques for Simulation Tools in Smart Grid

IET Journals
The Institution of Engineering and Technology

Multi-location virtual smart grid laboratory with testbed for analysis of secure communication and remote co-simulation: concept and application to integration of Berlin, Stockholm, Helsinki

ISSN 1751-8687
Received on 30th September 2016
Revised 2nd May 2017
Accepted on 2nd June 2017
E-First on 18th August 2017
doi: 10.1049/iet-gtd.2016.1578
www.ietdl.org

Christian Wiezorek[1] ✉, Alessandra Parisio[2,3], Timo Kyntäjä[4], Joonas Elo[4], Markus Gronau[1], Karl Henrik Johannson[2], Kai Strunz[1]

[1]*Faculty of Electrical Engineering and Computer Sciences, Technische Universität Berlin, Einsteinufer 11 (EMH-1), Berlin, Germany*
[2]*Department of Automatic Control, Kungliga Tekniska Högskolan, SE-100 44, Stockholm, Sweden*
[3]*Current affiliation: School of Electrical and Electronic Engineering, The University of Manchester, Ferranti C5, M13 9PL, Manchester, UK*
[4]*Teknologian tutkimuskeskus VTT Oy, FI-02044 VTT, Helsinki, Finland*
✉ *E-mail: christian.wiezorek@tu-berlin.de*

Abstract: The process of advancement and validation of smart grid technologies and systems calls for the availability of diverse expertise and resources. In response to this consideration, the virtual smart grid laboratory (VSGL) was developed as described in this study. At the core of the VSGL is a novel communication platform for seamlessly connecting geographically distributed laboratories with distinct competences. The platform has the dual purpose of opening access to resources of remote partner laboratory sites and offering the capability to emulate, analyse, and test smart grid communication networks involved in linking the distributed laboratory resources. The VSGL implementation is validated through a use case, in which the resources of R&D laboratories in three European countries are connected to form an aggregated system of distributed energy resources. The operation of the latter was coordinated through an energy management system based on model predictive control (MPC). The VSGL was found to be very suitable to meet the communication-specific requirements of such type of study. In addition, for this particular case the effectiveness of the MPC subject to diverse implementations of communication links was substantiated.

Nomenclature

c_{gas}	fuel cost for micro-CHP
$c_{\text{s},b}$	operating and maintenance cost related to power exchanged with storage unit for building b
c_{tariff}	electricity tariff
$E_{\text{s},b}(0)$	initial storage level for building b
$P_{\text{appliance},b}$	power of appliances profile for building b
P_b^{grid}	electrical power from electricity grid to building b
$\underline{P}_b^{\text{grid}}, \overline{P}_b^{\text{grid}}$	lower and upper bounds of P_b^{grid}
P_b^{heat}	thermal power demand for building b
$\underline{P}_b^{\text{heat}}, \overline{P}_b^{\text{heat}}$	lower and upper bounds of P_b^{heat}
$P_{\text{chp},b}^{\text{el}}$	micro-CHP electrical power to building b
$P_{\text{chp},b}^{\text{heat}}$	micro-CHP thermal power to building b
P_{gas}	gas power input to micro-CHP
$P_{\text{PV},b}$	power generated by renewables for building b
$P_{\text{running},b}$	power of appliances already running in previous time steps for building b

1 Introduction

The concept of the smart grid is closely tied to the management, processing, and exchange of comprehensive data. Even if decision-making procedures of system operation and control may be partly shifted to autonomously acting agents [1], distributed energy resources (DER) and loads heavily rely on knowledge about the system's present and future state to offer flexibility [2]. If possible, such information is made available in real time [3]. As a consequence, concepts for smart grid and aggregated systems of DER not only depend on intelligent data management and smart controls; however, also on fast, secure, and reliable communication [4, 5]. At the same time, to overcome additional hurdles for the implementation of smart grid technology, the underlying infrastructure should be flexible and affordable. It may integrate existing means of communication techniques and facilities, such as general-purpose networks [6] or power line communication [7, 8]. Determining a most suitable solution, also in terms of applied protocols and standards [9], can be challenging both from an economical and an application-specific point of view. While in some cases the deployment of state-of-the-art wireless technologies may be desirable [10, 11], other applications that require higher data rates and shorter delay times call for dedicated physical connections realised by co-axial cables or optical fibres. Furthermore, different types of data traffic constitute different requirements for the applied communication solution [12]. The availability of laboratory testbeds for the application-specific validation of smart grid communication can be very helpful in making decisions on technology choices.

A further challenge is the development of concepts and use cases in the area of smart grids and decentralised energy management systems (EMSs). A phase of dedicated simulation and testing prior to actual implementation helps to detect and prevent potential faults that can compromise services or security of supply. In this context, the integration of multi-energy concepts [13] as well as renewable and DER [14–16] becomes more important. The rising complexity of such systems and challenges in corresponding research and development make the access to diverse competence and resources very desirable. Thus, an interdisciplinary cooperation of laboratories appears promising – hence stimulating the proposed concept of pooling these laboratories.

The advantage offered by modern telecommunication in terms of amount and speed of data transmission over long distances support the fundamental idea of forming a virtual laboratory that can act as a single entity even though it comprises spatially separated sites. However, as with actual smart grid deployment, the

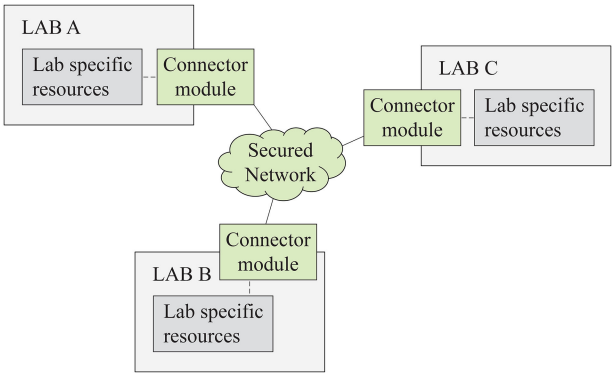

Fig. 1 *Superstructure of VSGL co-simulation environment integrating three geographically distributed labs*

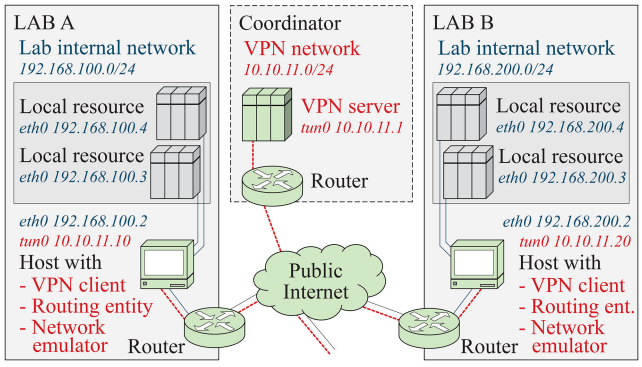

Fig. 2 *System architecture with VPN in star-topology coordinating the interconnectivity of distributed laboratory resources*

communication infrastructure needs to be dependable, secure, and flexible enough in order to support the laboratory operation. The solution presented in this paper aims to address key design challenges of a virtual smart grid laboratory (VSGL). For this purpose, a platform to provide the necessary framework for the quick and convenient set-up of co-simulation of remote laboratory resources was established. The platform is capable of assessing the quality of state-of-the-art telecommunication technologies for smart grid application.

The paper is organised as follows. In Section 2, the communication platform and its adaption to a VSGL co-simulation environment is described. The applied use case of a model predictive control (MPC)-based EMS is introduced in Section 3. In Section 4, the experimental conditions including the emulated network quality of service are outlined. In Section 5, the experience and results of both the applicability of the VSGL itself and the use case are presented and discussed. The paper closes with the conclusion in Section 6.

2 Communication platform for co-simulation environment

A superstructure of a co-simulation environment integrating the resources of three laboratories for close connectivity and interactivity among them is shown in Fig. 1. To assure confidential data exchange between the participating entities, the implementation of a secured network is essential, providing the backbone of the VSGL. Connector modules implemented at each laboratory need to perform the following fundamental tasks:

- Providing client and server functionality within the secured data distribution network.
- Adapting communication protocols in line with the VSGL application cases and the requirements of the laboratory resources, where necessary.
- Routing messages between the connected laboratories, and the physical and emulated resources within.

Ideally, the connector modules allow for intuitive integration of resources and extension of the VSGL. The design should enable non-experts in telecommunication to connect a laboratory site to the VSGL and to focus on the actual application.

In addition to the basic functionality of giving access to remote resources, the connector modules of the VSGL offer the possibility to evaluate the impact of different communication technologies and network conditions by emulating characterising features. Thus, the VSGL can be utilised to investigate both smart grid application cases from an energy-oriented perspective and for the qualification of diverse communication technologies as part of these application cases.

In the following subsection, the secured network for data distribution and the routing mechanisms are described. Then, the communication protocol integration and the messaging are characterised. In the final subsection, the emulation of telecommunication network technologies is explained in detail.

2.1 Data distribution with secured private network

An important feature of the VSGL is provided by the establishment of a private network necessary for the secure interconnectivity between the distributed laboratories. Instead of requiring dedicated lines, this network can be placed on top of the public Internet or local area networks. The system architecture is depicted in Fig. 2. The secured network is provided by establishing a virtual private network (VPN), using open-source OpenVPN software [17], and assuring both required information security and message integrity. A VPN server, running at a dedicated location in the network, coordinates the entire traffic between the interconnected laboratories. The VPN server is configured using encrypted User Datagram Protocol (UDP) VPN tunnels in a star topology, thus creating the client-to-client environment where clients can connect, communicate, and share local resources with each other. The VPN clients, as part of the connector modules, are installed on host machines within the connected laboratories.

As a distinctive feature of the VSGL data distribution system, the main networking mechanisms are implemented at different layers in the TCP/IP model. The VPN, using the SSL/TLS, is located between the transport and application layers, as described in Table 1 in Section 2.2. In contrast, parts of the routing mechanism are located in the application layer directly. This concerns in particular the routing of messages between those application-specific laboratory resources whose physical location in the laboratory differs from the location assumed in the use case. Since all relevant information pertaining to the use case is kept at the application layer, there is no need for the user to have knowledge on the lower network protocol layers. Instead, a routing entity, designed as part of the connector module installed at each laboratory, parses routing information to local resources given directly in the application layer message. The parsing is based on initially created routing tables and configuration files. This way, the VSGL can be quickly adapted to new application cases without expert knowledge on network protocols.

2.2 Messaging and protocol integration

A lightweight protocol with a simple custom message structure was applied in favour of considering more complex application layer standards such as IEC 61970 or 61850. Each connected local laboratory resource, whether physical or virtual, is given a specific ID. In the message header on the application layer level, the IDs of sending and receiving entities are registered. Also given are the message type in the application context and a time stamp in the case that the experimental set-up includes non-real-time simulation. The format of the actual message body is not restricted and, thus, can be adapted to the application the VSGL is used for.

To map the data messages to the actual laboratory resources, protocol adapters at the interface between the routing entity, as described in Section 2.1, and the local resources are applied. In the case of the laboratories in Berlin and Stockholm, where the local resources are controlled from the Matlab environment, this adaptor was implemented as shown in Fig. 3*a*. The adaptor consists of a socket-based client server communication, a configurable message

Table 1 Overview of applied communication protocols

Layer	Protocol	Description
application	custom	local resource routing,
	OPC UA	APROS communication,
	NTP	virtual lab time synchronisation,
	SSH	virtual lab management.
presentation	Telnet	application protocols adaption,
		openVPN management.
session	Sockets	routing entity communication.
transport	TLS/SSL	asymmetric cryptographic auth.,
	TCP/IP	routing entity communication,
	UDP	openVPN tunnels
network	IPv4	relaying datagrams across network, network
	ICMP	delay measuring
data link	Ethernet	transmission of data frames,
	AES	OpenVPN encryption
physical	IEEE	transmission and reception of raw bit streams
	802.3	over physical medium

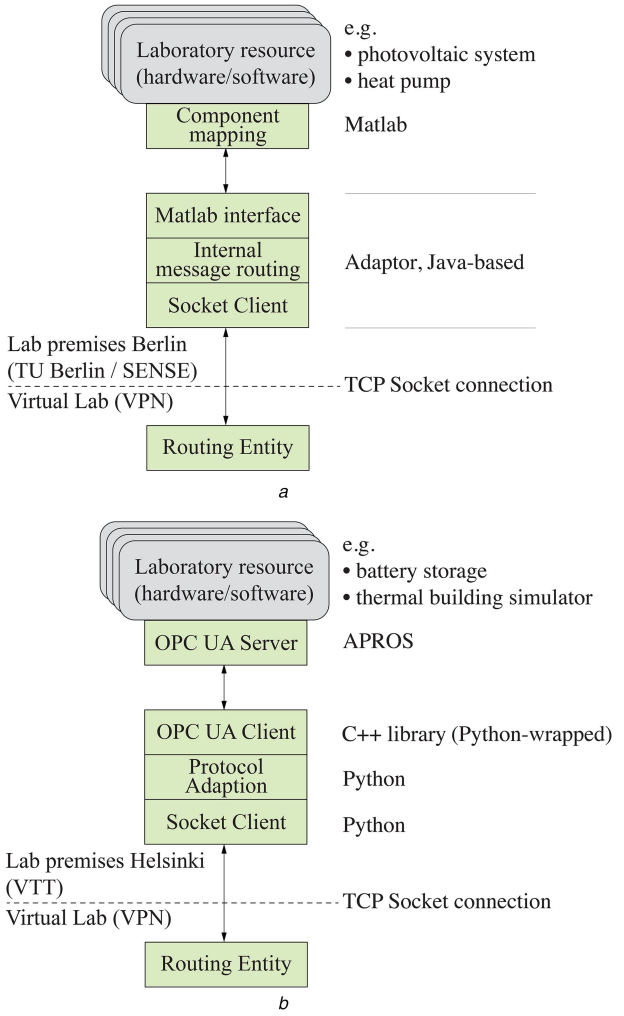

Fig. 3 *Protocol adaption and component mapping to* **(*a*)** Matlab environment (TU Berlin and KTH Stockholm), **(*b*)** APROS environment communicating with OPC UA protocol (VTT Helsinki)

routing module, and an interface to Matlab. While acting either as a network server or a client, the communication module receives data from external laboratories and allows executing Matlab functions on the received input data in order to control or simulate local resources. Likewise, data received from Matlab can be sent to external resources in the VSGL. In the case of a connection loss or high network latency, the adaptor buffers outgoing data and connects autonomously and continuously to the other VSGL parties.

All parts of the adaptor are highly customisable through a dedicated configuration interface and allow the reception and transmission of single values but also time series of forecasts, actual quantities, and set points. The application is written as a platform-independent component in the Java programming language, using standard libraries and imposing only a small memory and CPU footprint. The implementation based on the Java Matlab Interface provides a generic configurable interface independent of applied platforms, machines, ports or message content.

The laboratory in Helsinki connects resources provided by the APROS system, a proprietary software environment for process simulation [18]. APROS is optimised for communication via the OPC UA protocol. OPC UA, an industrial M2M communication standard, is a widely used communication and system integration protocol for automation, Industrial Internet, Industry 4.0 and Internet of things, integrating all the functionality of individual OPC specifications into one extensible framework without platform dependency [19]. To connect the APROS system to the VSGL, an additional protocol adaptor is implemented to translate between the TCP-based socket connection using text-based protocols and the OPC UA client linking to APROS. The protocol integration and mapping of resources at the Helsinki laboratory is depicted in Fig. 3*b*. In contrast to the laboratories using the Matlab environment, the integration makes use of the Python programming language and C++ libraries.

In Table 1, the Virtual Lab communication platform is expressed in terms of the Open Systems Interconnection model. This provides an understanding at which layer level the respective protocols come into effect.

2.3 Telecommunication network emulation

The telecommunication network emulator is part of the connector module implemented at the connected laboratories' clients, as shown in Figs. 1 and 2 in Section 2.1. It is open source-based software for emulating heterogeneous real-world network conditions on normal best-effort networks by manipulating network interface parameters. With the emulation of different types of real life connections, it is, e.g. possible to test if the desired communication link is able to meet the requirements of the smart grid application in question. The network emulator is also capable of emulating real time alterations in telecommunication links in order to find answers to the following questions:

- How is a heavy congested network with a substantial loss of data packages handled? Is the system able to recover after the link has returned to normal conditions?
- What happens in case of high dynamics where the bandwidth is decreased or increased in a short period of time? Can the system adapt to this kind of changes?
- How does these network conditions influence the VSGL application case? Can co-simulation specific mechanisms prevent application failures?

In addition to providing manipulating capability of standard physical network interfaces, the network emulator can also handle virtual network interfaces. In this manner, it can be used in physical machines as well as in virtual machines, and thus, also supports other types of automation systems, such as: simulators, applications, and physical devices. An example use case including virtual networks is illustrated in Fig. 4*a*, where the interface between a simulation engine and an entity using OPC UA is emulated as virtual link.

The manipulating capabilities of the network emulator address parameters required for the characterisation of state-of-the-art telecommunication technologies. Most importantly, bandwidth and speed of data transmission can be limited according to technology-specific constraints. The delay between sending and receiving of messages, especially important for connections between remote entities and for mobile communication in general, can be

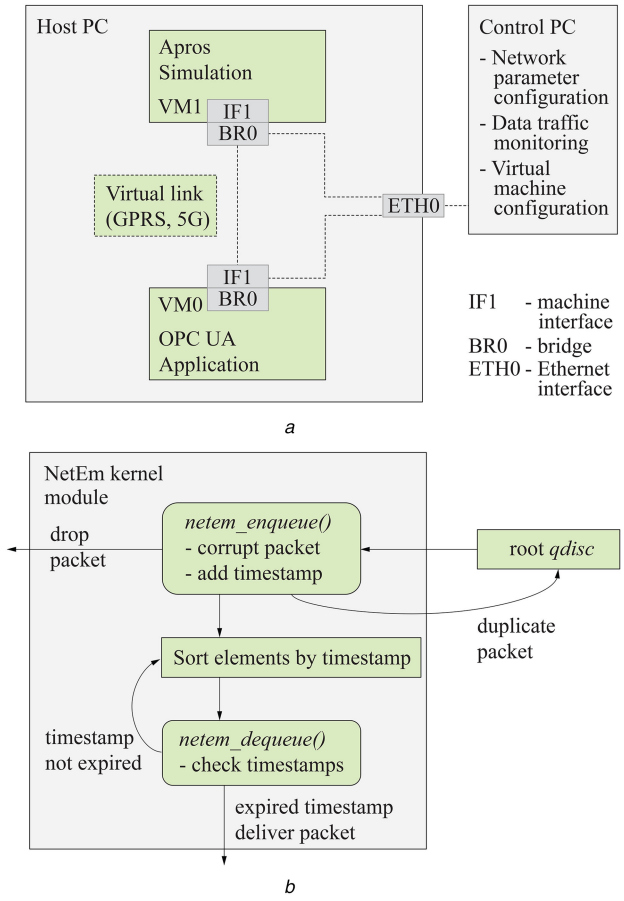

Fig. 4 *Network emulation*
(***a***) Simple demonstrator, (***b***) Flowchart of data packet manipulation using NetEm kernel module

Table 2 Description of network emulation parameters with example configuration

Parameter	Value	Description of impact
		Bandwidth
up traffic	256	limits outgoing traffic to 256 kb/s.
down traffic	256	limits incoming traffic to 256 kb/s.
delay	200	causes added delay to be 200 ms ± 20 ms with the next random element depending 25% on the last one.
variation	20	
correlation	25	
		Packets
loss	0.5	causes 0.5% of packets to be randomly dropped where each successive probability depends by a quarter (25%) on the last one.
correlation	25	
duplication	0.1	causes 0.1% of packets to be duplicated before queuing them.
corruption	0.1	causes 0.1% of packets to have single bit error at random offset.
reorder	0.5	causes 0.5% of packets to be sent in disorder with 30% correlation.
correlation	30	

manipulated to a different time value. This also accounts for delay variations and delay correlation of sequentially sent data packages. Other features manipulate the data packages, including loss and duplication of packages, as well as corruption and reordering of data. An overview of the manipulation extent is given in Table 2, providing an example configuration.

The actual network traffic shaping is handled by using the Linux Network Emulator (NetEm) functionality [20], consisting of two individual components, a tiny kernel module for a queuing discipline (qdisc) and a command-line tool for configuration. The processing principles of emulation including the manipulation of data packages according to the previously expounded characteristics are drawn schematically in Fig. 4*b*.

3 Resources and energy management system

An EMS for the coordinated optimal operation of DER and flexible household loads, based on MPC, was implemented and tested within the VSGL. For this application three European smart grid research laboratories were connected:

- The Smart Grid Laboratory of the Chair of Sustainable Electric Networks and Sources of Energy (SENSE) of TU Berlin, a power hardware-software-based laboratory for R&D on design, operation, and control of smart grids and integration of renewable energy [21].
- The testing facilities of the Networked Control Systems Group at Kungliga Tekniska Högskolan (KTH, Royal Institute of Technology), Stockholm, focusing on control of multi-agent and embedded systems, wireless sensor actuators and networks, and SCADA systems.
- The facilities of the Self-organising Networks Group of Teknologian Tutkimuskeskus VTT Oy (VTT, Technical Research Centre of Finland), Helsinki, developing intelligent communication technology for the growing need for efficient and reliable communication systems.

Each participant's laboratory provided both specific resources for connection to the VSGL and the DER required for modelling the energy system of interest.

3.1 Modelling of DER and flexible loads

The architecture of the application model implemented in the VSGL is depicted in Fig. 5. The power hardware comprises a set of DER including storage and conversion units as well as flexible consumer loads. An upper-level EMS coordinates the overall system operation. Local controls at the level of a building act on local DER and load devices. The overall model includes the coupling of electricity and thermal energy by integrating heat pumps (HP) and a distributed combined heat and power (CHP) conversion unit. Photovoltaics (PV) is included and combined with battery energy storage systems (ESS). Flexible domestic loads are provided by smart electric appliances capable of acting upon demand response signals. The heating system can take advantage of the buildings' thermal inertia and of a certain range of user comfort level. The system is connected to the electric power grid and natural gas network. It is so able to receive power as well as to feed in surplus power generated by the PV systems and the micro-CHP.

The optimisation underlying the EMS aims for a coordinated system operation at the lowest total operational cost. It makes use of the degrees of freedom provided by the flexible resources while also complying with given constraints. The optimisation developed for the EMS relies on the technique of MPC. The MPC computes setpoints for the energy resources and end-user smart appliances based on the current and predicted state of the system. Using time-varying prices as signals for purchasing and selling of energy, the EMS controls the interaction with the electric power and natural gas network. The modelling and MPC problem formulation are detailed below [22].

The flexible resource models are allocated based on the members' laboratory hardware availability. The EMS, the micro-CHP and the smart appliances are resources of KTH; TU Berlin connects the PV system and HP; domestic heating and batteries are provided by VTT's APROS simulation environment [18].

3.1.1 Electrical and thermal loads: Two types of flexible loads are considered: thermal loads as a function of demand levels related to a thermal indoor comfort range, and electrical loads that are given by the demand of smart domestic appliances.

Thermal loads. On the basis of forecasts of the weather conditions, the forecasts of minimum and maximum thermal energy required to keep the buildings' indoor temperature within a

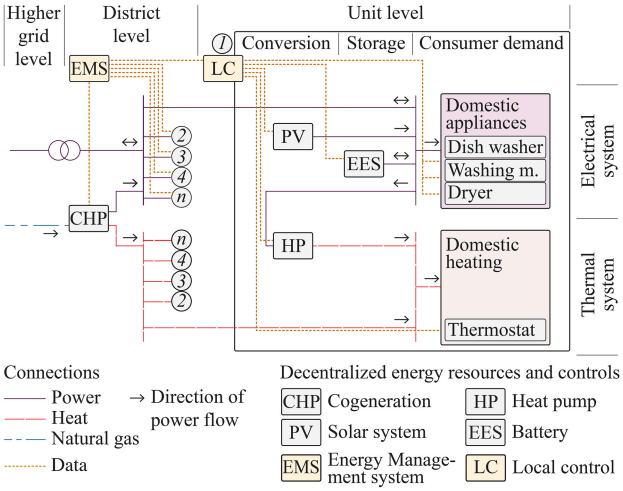

Fig. 5 *Architecture of energy system model and connectivity for communication*

given comfort range are computed using a dynamic thermal building model. The model runs on top of VTT's APROS process simulation software [18]. It includes energy dynamics dependent on the building structure and indoor temperature level. It accounts for the outdoor temperature, the solar radiation, and the internal heat gains from occupants and equipment.

Electrical loads. The operational processes of the appliances consist of several sub-processes referred to as energy phases. An energy phase is considered uninterruptible, describing the conversion of a predefined amount of energy in order to finish the respective physical task. Furthermore, several technical and user specific constraints are included in the problem formulation. First, both the power profile assigned to the energy phase at any time slot and its duration have to adopt values within a specified range. Second, all energy phases associated with a single appliance must be run sequentially. Third, delays between the energy phases are considered; but the required order of several appliances coupled by usage, for instance washing machines and clothing dryers, must be kept. Fourth, for safety and capacity reasons, the total power assigned to all appliances at any moment cannot exceed a certain limit. Fifth, user-specified time preferences are included, requiring that certain appliances need to be run within particular time intervals. Sixth, additional user-specified preferences on combined appliance usage are considered, e.g. a certain appliance cannot start before some other appliance finishes. Further details on modelling of appliances and electrical loads may be found in [23].

3.1.2 Electrical energy storage: For a storage unit linked to a certain building b, the following discrete time model is considered:

$$E_{\mathrm{s},b}(k+1) = \alpha_{\mathrm{s},b} E_{\mathrm{s},b}(k) + \eta^{\mathrm{c}}_{\mathrm{s},b} P^{\mathrm{c}}_{\mathrm{s},b}(k)\tau - \eta^{\mathrm{d}}_{\mathrm{s},b} P^{\mathrm{d}}_{\mathrm{s},b}(k)\tau \tag{1}$$

with $E_{\mathrm{s},b}(k)$ indicating the storage energy level for building b at time step k, $0 < \eta^{\mathrm{c}}_{\mathrm{s},b} < 1$ and $0 < \eta^{\mathrm{d}}_{\mathrm{s},b} < 1$ accounting for the efficiencies during charging (c) and discharging (d), $\alpha_{\mathrm{s},b}$ accounting for self-discharge losses, $\tau = t_{k+1} - t_k$ is a constant time step size, $E_{\mathrm{s},b}(k)$ is the storage energy level for building b at time step k, $P^{\mathrm{c}}_{\mathrm{s},b}(k)$ and $P^{\mathrm{d}}_{\mathrm{s},b}(k)$ are the charging and discharging power exchanged with the storage of building b at time step k.

The state of charge (SOC) of the battery is defined as follows:

$$\mathrm{SOC}_{\mathrm{s},b}(k) = \frac{E_{\mathrm{s},b}(k)}{E^{\mathrm{n}}_{\mathrm{s},b}} \tag{2}$$

where $E^{\mathrm{n}}_{\mathrm{s},b}$ gives the nominal capacity of the battery.

Binary variables $\delta^{\mathrm{c}}_{\mathrm{s},b}$, $\delta^{\mathrm{d}}_{\mathrm{s},b}$ are introduced to identify the charging and discharging behaviour and to rule out the possibility of having charging and discharging during the same sampling period, as expressed by the following constraints:

$$\begin{aligned} P^{\min}_{\mathrm{s},b}\delta^{\mathrm{c}}_{\mathrm{s},b}(k) &< P^{\mathrm{c}}_{\mathrm{s},b}(k) < P^{\max}_{\mathrm{s},b}\delta^{\mathrm{c}}_{\mathrm{s},b}(k) \\ P^{\min}_{\mathrm{s},b}\delta^{\mathrm{d}}_{\mathrm{s},b}(k) &< P^{\mathrm{d}}_{\mathrm{s},b}(k) < P^{\max}_{\mathrm{s},b}\delta^{\mathrm{d}}_{\mathrm{s},b}(k) \\ \delta^{\mathrm{c}}_{\mathrm{s},b}(k) + \delta^{\mathrm{d}}_{\mathrm{s},b}(k) &\le 1 \end{aligned} \tag{3}$$

where $P^{\min}_{\mathrm{s},b}$ and $P^{\max}_{\mathrm{s},b}$ are bounds on the power exchanged with the storage of building b. Bounds on the storage capacity are included in the modelling, along with limits on the total number of daily charging and discharging cycles in order to take the state of health of the EES into account.

3.1.3 Photovoltaic system: The PV model calculates the electric power output based on both the irradiance on the solar panels and the change of conversion efficiency subject to operational conditions. First, the irradiance of the general weather data is transformed into irradiation received on the tilted panel surfaces based on the algorithm provided by the German Institute of Standardisation DIN [24]. Then, the power output is calculated according to the following equations:

$$\begin{aligned} P_{\mathrm{PV},b}(k) &= I_{E,\mathrm{PV}}(k) \cdot A_{\mathrm{PV},b} \cdot \prod_{i=1}^{3} \eta_i \\ \eta_1 &= 1 - (T_{\mathrm{PV},b}(k) - T_{\mathrm{STC}}) \cdot f_{\eta,\mathrm{T}} \\ \eta_2 &= log\left(\frac{I_{E,\mathrm{PV}}(k)}{f_{\eta,E,1}}\right)^{f_{\eta,\mathrm{E},2}} \\ \eta_3 &= \eta_{\mathrm{lump}} \end{aligned} \tag{4}$$

with $I_{E,\mathrm{PV}}(k)$ giving the received area-specific solar irradiance on the panel surface at time step k, $A_{\mathrm{PV},b}$ is the active panel area of building b, $T_{\mathrm{PV},b}(k)$ is the temperature of PV panels of building b at time step k, T_{STC} is the panel temperature under standard test conditions (STC), $f_{\eta,\mathrm{T}}$ is the installation-specific temperature modification factor, and $f_{\eta,E,1}$ and $f_{\eta,E,2}$ are the technology-specific irradiance modification factors. The efficiency factor η_{lump} accounts for additional sources of losses, for instance losses of inverters and cables. The values for $f_{\eta,\mathrm{T}}$ are obtained from PV panel manufacturers' data sheets, $f_{\eta,E,1}$ and $f_{\eta,E,2}$ are calculated based on resources provided by the PVsyst tool [25], and the optimum tilt and alignment of PV panels are taken from the Photovoltaic Geographical Information System (PVGIS) [26].

3.1.4 Co-generation system: The component represents a typical small CHP (micro-CHP) unit. The modelling of the component adopts a data-driven approach, where data from a real-world deployment were used [22]. The micro-CHP model is:

$$\begin{aligned} P^{\mathrm{el}}_{\mathrm{chp}}(k) &= \alpha_1 \cdot P_{\mathrm{gas}}(k) + \alpha_0 \\ P^{\mathrm{heat}}_{\mathrm{chp}}(k) &= \beta_1 \cdot P_{\mathrm{gas}}(k) + \beta_0 \end{aligned} \tag{5}$$

where $P^{\mathrm{el}}_{\mathrm{chp}}(k)$, $P^{\mathrm{heat}}_{\mathrm{chp}}(k)$, and $P_{\mathrm{gas}}(k)$ are micro-CHP electrical and thermal power outputs and gas power input to the micro-CHP at time step k, respectively. The coefficients α_0, α_1, β_0 and β_1 are determined by analysing measurements over long periods of CHP operation, applying state-of-the-art machine learning techniques.

3.1.5 Heat pump: Electrically operated HP using ambient air as heat source are used here since this type is by far the most frequently used. As the thermal efficiency of heat pump systems strongly depends on the temperature difference between heat source and sink as well as the overall operating temperature level, forecasts of the coefficient of performance (COP) based on temperature predictions are integrated in the proposed control framework. This allows to predict the future heat generated by each heat pump. The behaviour of the heat pump at each time step k and for each building b is given by:

$$P^{\text{heat}}_{\text{hp},b}(k) = \text{COP}_{\text{hp},b}(k) \cdot P^{\text{el}}_{\text{hp},b}(k) \tag{6}$$

where $\text{COP}_{\text{hp},b}$ is the forecasted efficiency factor based on weather forecasts, and $P^{\text{heat}}_{\text{hp},b}(k)$ and $P^{\text{el}}_{\text{hp},b}(k)$ are thermal power output and electrical power input at time step k, respectively. The implemented model is based on COP measurements for air HP conducted by the German Energy Research Centre BINE [27].

3.2 MPC based energy management

The EMS provides the optimal energy dispatch for each controllable DER and load using weather and power generation forecasts. The optimisation algorithm based on MPC calculates the resource setpoints using a floating planning horizon of 24 h in advance. The iterative process takes forecasting errors into account. Corrective actions and the corresponding costs are considered in order to cope with potential imbalances.

With the beginning of each sampling period, the EMS sends forecasted weather data such as irradiance, ambient temperature, and wind speed for the entire planning horizon to the local controls of the weather-sensitive subsystems like PV, HP, and building heating systems. In response, the local control systems calculate and send back forecasted generation and load profiles. At the same time, the EMS receives updated status messages of controllable devices including the storage systems and the smart appliances. Having the necessary information and external day-ahead pricing available, the MPC algorithm of the EMS calculates the optimal schedule. The resulting setpoints for power inputs and outputs of controllable DERs as well as the starting times for flexible loads are sent to the respective devices.

The optimisation problem is formulated as the minimisation of operation costs subject to energy purchase and sale of excess electricity within the whole planning horizon. At each time step k, given an initial state of storage for each building b $E_{\text{s}}(k) = [E_{\text{s},1}(k), \ldots, E_{\text{s},B}(k)]$, the MPC scheme solves the following optimisation problem:

$$\begin{aligned} J(E_{\text{s}}(k)) = \min \sum_{k=0}^{H-1} \Bigg[\sum_{b=1}^{B} \Big(& c_{\text{tariff}}(k) P^{\text{grid}}_{b}(k) \\ & + c_{\text{s},b}(P^{\text{c}}_{\text{s},b}(k) + P^{\text{d}}_{\text{s},b}(k)) \Big) + c_{\text{gas}} P_{\text{gas}}(k) \Bigg] \tau \end{aligned} \tag{7}$$

where B is the number of buildings and H is the prediction horizon. This problem is subject to operational constraints of the controllable DER, provided by (3), (5), and (6), and the following equations:

$$P^{\text{heat}}_{b}(k) \;=\; 0.7 P_{\text{running},b}(k) + P^{\text{heat}}_{\text{hp},b}(k) + P^{\text{heat}}_{\text{chp},b}(k) \tag{8}$$

$$\begin{aligned} P^{\text{grid}}_{b}(k) = {} & P_{\text{appliance},b}(k) + P_{\text{running},b}(k) + P^{\text{c}}_{\text{s},b}(k) \\ & - P^{\text{d}}_{\text{s},b}(k) + P^{\text{el}}_{\text{hp},b}(k) - P^{\text{el}}_{\text{chp},b}(k) - P_{\text{PV},b}(k) \end{aligned} \tag{9}$$

$$\underline{P}^{\text{heat}}_{b} \;\le\; P^{\text{heat}}_{b}(k) \;\le\; \overline{P}^{\text{heat}}_{b} \tag{10}$$

$$\underline{P}^{\text{grid}}_{b} \;\le\; P^{\text{grid}}_{b}(k) \;\le\; \overline{P}^{\text{grid}}_{b} \tag{11}$$

Table 3 Main parameters of DERs

	Technology type	Maximum performance	Nominal efficiency
CHP	solid oxide	20 kW (el)	39.2%
	fuel cell	25 kW (th)	49.0%
PV	mono-crystalline	1 kWp	15.7%
battery	lead-acid	1 kWh	72.3% (RT)
heat pump	air-water	2 kW (el)	COP of 3

$$\sum_{b=1}^{B} P^{\text{el}}_{\text{chp},b}(k) = P^{\text{el}}_{\text{chp}}(k) \tag{12}$$

$$\sum_{b=1}^{B} P^{\text{heat}}_{\text{chp},b}(k) = P^{\text{heat}}_{\text{chp}}(k) \tag{13}$$

where (8) and (9) account for the balance of thermal power and electrical power, respectively; (10) keeps the heat provided to each building within the thermal power demand bounds and (11) defines the capacity limits of the coupling point to the external power network, subject to the operator's service conditions; (12) and (13) ensure that the electrical and the thermal power outputs of the micro-CHP equal the sum of shares among the buildings. The first term in the thermal balance in (8) accounts for the waste heat generated by running appliances; studies suggest that 70% of regular electric use contributes to the building's heat demand [22]. Parameters and variables included in the MPC problem are reported in the Nomenclature section. The control algorithm was implemented as mixed integer linear program (MILP) in the Matlab environment, using ILOG's CPLEX 12.0 [28] with branch and bound techniques.

4 Experimental set-up

The developed EMS was tested in a Virtual Lab co-simulation addressing two objectives. The first objective was concerned with the performance of the MPC algorithm in terms of the optimisation goal. The second objective was to determine the impact of communication network conditions on the EMS performance.

4.1 Set-up of EMS performance evaluation

The EMS and the underlying MPC algorithm are evaluated through a case study in which the influence of storage availability on the control strategy and the reduction of operational costs are investigated. The case study considers a system of five buildings and a shared CHP system rated at 20 kW electric and 25 kW thermal power output, located in the Stockholm area. Each building is equipped with a small 1 kWp PV system as well as a heat pump of 2 kW rated electric power. The heat pump is able to supply peak heating loads not covered by the co-generation plant. The buildings' indoor temperature range in the heating period is defined between 20 and 24°C to meet the inhabitants thermal comfort [29]. The flexible smart appliances in each building comprise washing machines, dryers, and dishwashers. These appliances are scheduled considering user specific time preferences and certain constraints, e.g. dryers are not to be started before washing cycles are finished. Furthermore, the case study makes reference to the modern Stockholm Royal Seaport (SRS) urban district [30] by including a building representative for SRS-specific average hourly power consumption and scheduling of appliances.

Two different application cases were evaluated: In the first case, no energy storage is available. In the second case, each building is equipped with a 1 kWh battery providing additional flexibility. The main characterising parameters of each system component are listed in Tables 3 and 4. For the use of each flexible appliance, Table 4 lists event-specific values such as number of energy phases, as defined in Section 3.1.1, the total energy use during the operation time, and the operation time itself.

The simulation horizon is set to one month. In particular, all external input data for weather, electricity prices, and photovoltaic generation refer to November 2014. The weather data were collected from an actual weather station located in Östermalm, a district in Stockholm's city centre, whereas the electricity prices refer to data of the Nordic market Nordpool for the Stockholm area. The natural gas price information was received from Eurostat.

4.2 Set-up of telecommunication network evaluation

From the communication point of view, with a growing number of flexible local energy resources commonly controlled by an EMS, the networking infrastructure needs to be adapted. In this context,

the impact of certain network constraints on the EMS performance was tested, using the network emulator included in the VSGL. A reference scenario, in the following referred to as scenario 1, and three additional network scenarios were analysed. In scenario 1, only the actual network conditions of the public Internet connections were applied. This scenario is affected by conditions beyond the VSGL, including:

- conditions of inter and intra-country links,
- policies of national operators providing the connections,
- service level agreements of each host site operator,
- the amount of communication data at each time.

The experienced network quality of service can improve or decrease occasionally. Therefore, the conditions of scenario 1 are neither controllable nor predictable. Starting from the reference scenario, the EMS co-simulation was executed repeatedly with three additional scenarios addressing common communication technologies and network conditions. Scenario 2 emulates a 'highly restricted bandwidth', as it still is assumed to rely on 3G technologies. Scenario 3 considers a 'reduced cost service', subject to a lower service level agreement of the host site operator. Scenario 4 reproduces a network with a 'locally congested connection', drastically increasing the delay and loss of data packages. The applied parameters of scenarios 2 to 4 are listed in Table 5.

5 Results and discussion

In the following, the performance of both the VSGL communication platform and the EMS is analysed and discussed. The evaluation is based on the measurement of VSGL communication performance indicators and the optimisation results achieved by the MPC algorithm.

5.1 Analysis of communication platform

With focus on the communication network, two different sets of measurements were conducted. First, the ability of the VSGL to serve as a secure and reliable environment for co-simulation involving distributed laboratories was tested. Then, the performance of the telecommunication links with emulated network restrictions was investigated.

5.1.1 Virtual smart grid laboratory platform: The communication platform of the VSGL was tested in terms of its capability to provide a suitable environment for co-simulation and network emulation. The most important requirements of the communication infrastructure are robustness, a low latency, and high throughput between the laboratory partners. A convincing base performance with a latency of less than 100 ms and a throughput of more than 30 Mb/s would allow for flexibility for the emulation of additional restrictions necessary for follow-up impact testing.

In a first stage of verification, the round-trip time (RTT) latency between pairs of connected laboratories was measured with and without the application of the VPN, using simple ICMP Echo requests with 84 Byte IP packet size. To take into account possible latency variations related to date and time, the measurements were repeated each minute over the course of one week, resulting in 10,800 values in total. The supplemental VPN network latency, in addition to the one of the public Internet, was very minor, as can be seen in Fig. 6*a*. Within the scope of the use cases, it is insignificant and thus can be neglected. The total round-trip latencies, summarised in Fig. 6*b*, are <100 ms in each intercity connection. The values reveal an almost linear correlation to the distance between the connected laboratories. The distance of Berlin – Helsinki is 1,100 km, for Stockholm – Helsinki it is 400 km, and Stockholm – Berlin is about 810 km.

Second, the throughput and quality of the network links were measured using the iperf2 network-testing tool. The maximum throughput was quantified using bi-directional TCP connection with a window size of 85.3 kByte, whereas jitter and datagram losses were measured using UDP connection with a 1,470 Byte datagram size. The test durations were set to 100 s, using measurement intervals of 10 s. In order to eliminate possible inaccuracies and momentary variations in measurements, the tests were repeated twice a day for one week. The average jitter was measured to vary from 0.049 to 0.175 ms, whereas the packet loss in links was less than 0.01% in total. The average throughput was not <50 Mb/s in any case, as summarised in Fig. 6*c*.

5.1.2 Network emulation: The network emulation on top of the actual communication link performance was successfully implemented with the three additional network scenarios as defined in Table 5. The measurements of RTT latency and throughput, as explained in Section 5.1.1, were repeated. The results, summarised in Figs. 7 and 8, show network performances in line with the scenario definitions and also reveal interesting details.

As expected, the RTT latency largely increased, especially in scenario 4 representing a highly congested network with a large delay and data package losses, see Fig. 7*d*. The variation in latency

Table 4 Main parameters of flexible loads per event with respect to all energy phases

	Number of energy phases	Energy use, total, Wh	Min. power, W	Max. power, W	Operation time, min
dish-washer	6	1,360	2.3	2,143	132.1
washing machine	8	2,346	5.0	2,200	162.7
dryer	1	2,426	120.5	1,454	120.8

Table 5 Applied network scenarios on top of reference scenario 1

	Scenario 2	Scenario 3	Scenario 4
scenario focus	highly restricted bandwidth	reduced cost service	locally congested connection
technology scope	3G	4G/5G	4G/5G
bandwidth up, kb/s	256	5,000	1,000
bandwidth down, kb/s	256	5,000	1,000
delay, ms	200	50	200
delay variation, ms	± 50	± 30	± 150
delay correlation, %	0	0	0
packet loss, %	0.5	0.5	5
loss correlation, %	0	0	50
duplication, %	0.1	0.1	0.1
corruption, %	0.1	0.1	0.1
reorder, %	0.2	0.2	0.2
reorder correlation, %	0	0	0

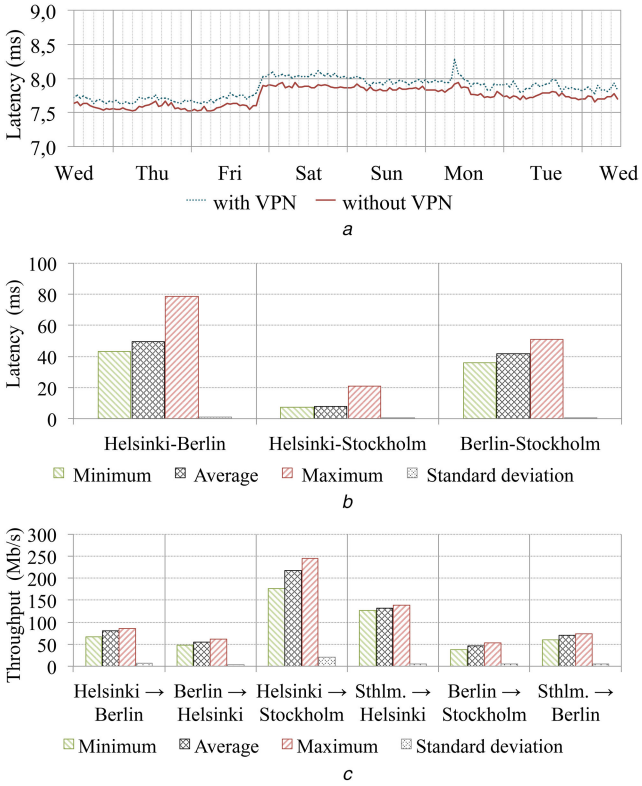

Fig. 6 *Communication platform performance*

(*a*) Course of round-trip latency for one week between Stockholm and Helsinki with and without VPN, **(*b*)** Summary of round-trip latency for all connections, **(*c*)** Summary of throughput for all connections

Fig. 7 *Latency measurements for network emulation*

(*a*) Reference scenario 1 without emulated links, **(*b*)** Scenario 2 'Highly restricted bandwidth', **(*c*)** Scenario 3 'Reduced cost service', **(*d*)** Scenario 4 'Locally congested connection'

for this case is much higher than for scenario 2 with the emulated 3G links, as shown in Fig. 7*b*. Scenario 2 results in similar average values, but no peak does exceed 1,000 ms. The performance of the communication link in scenario 3 with moderate values for delay and package losses is better, as shown in Fig. 7*c*. It is even close to the reference scenario, depicted in Fig. 7*a*. Interestingly, for the reference scenario 1, the performance of the connection between Berlin and Stockholm is the worst compared with the performance of the other connections. However, with the network emulation, the RTT latency of this link is, in any case, lower than for the links connecting Helsinki.

In terms of the overall throughput, the performance of the emulated networks was highly reduced, compared with reference scenario 1. In particular, this concerned the links in scenario 2 representing 3G technology, as can be seen in Fig. 8*b*. As expected, in scenario 3 the network delivers the best performance of all scenarios with emulated links, as illustrated in Fig. 8*c*. The overall poor performance of the scenario 4 data links, as shown in Fig. 8*d*, is a consequence of the emulated network congestions. The performance of the Berlin-Stockholm link is remarkably better than the ones of the other connections, also in the reference scenario 1. Only in scenario 2, the throughput is of the same order of magnitude for each connection. It is highly restricted by the emulated bandwidth boundary of 3G technologies.

5.2 Analysis of the EMS co-simulation results

The performance of the EMS is evaluated in two respects. First, the results of the two EMS application cases for controlling a system with and without storage are compared. Then, the impact of the different communication network scenarios on the EMS performance is analysed and discussed.

5.2.1 EMS performance as a function of EES availability: The EMS operates the system as illustrated in Fig. 5. It includes the DERs listed in Table 3 and the flexible domestic appliances whose event-specific parameters are summarised in Table 4. By considering the results for the two different application cases of a system with and without installed battery storage, the effectiveness of the MPC-based EMS can be compared. In particular, building #4, representing a typical housing unit in the Stockholm Royal Seaport area, exhibits the most significant benefit when using an EES. In contrast to the other buildings with only minor flexibility in load scheduling, the Stockholm Royal Seaport building is able to avoid a significantly larger number of electricity price peaks. The application of additional peak shifting capacity provided by the EES contributes to this effect.

As depicted in Fig. 9*a*, showing the progression of the battery's SOC on the 13th day of the simulated month of November, the EES is operated in correlation with electricity prices: it is charged in times of lower prices and discharged when electricity prices are high. Owing to the seasonally typically low solar irradiance conditions, PV power generation barely affects the storage levels. With respect to the power exchanged with the grid, the application of EES leads to a more flattened profile, as shown in Fig. 9*b*; in particular a remarkable peak shaving is achieved during the first 168 h, with respect to the scenario without EES. In consequence, the running time of the smart appliances becomes less sensitive to the electricity price profile, and the EMS can activate them also when prices are higher. Furthermore, the application of battery storage allows for a less volatile electrical power output from the shared micro-CHP. This benefits both the efficiency and the lifetime of the co-generation system.

Summarising the EMS performance, the energy cost for the one-month operation is 81.29 € in total for the scenario without

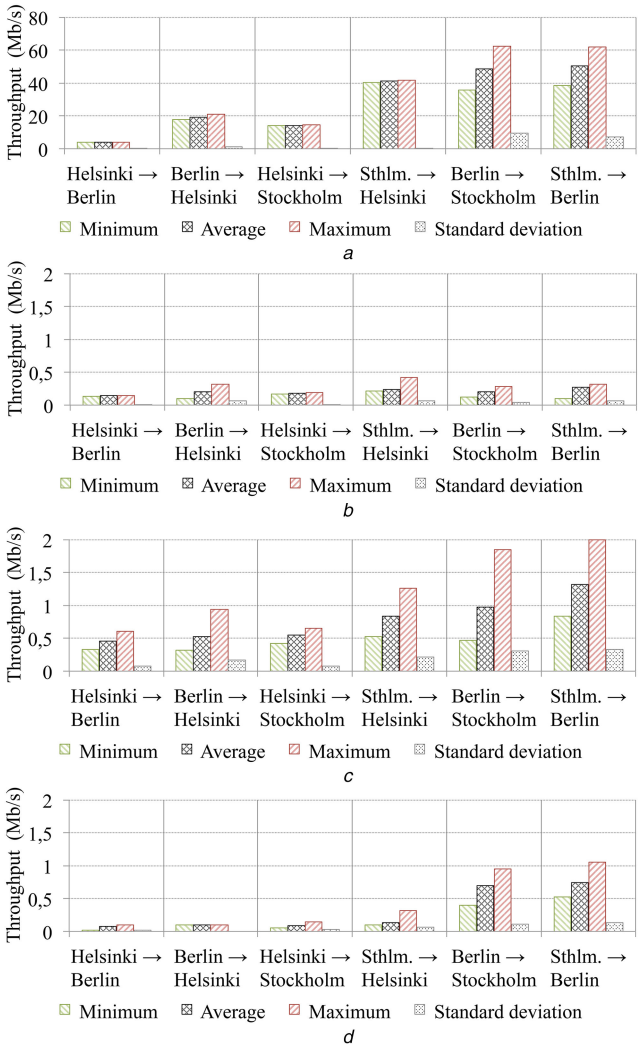

Fig. 8 *Throughput measurements for network emulation*
(*a*) Reference scenario 1 without emulated links, **(*b*)** Scenario 2 'Highly restricted bandwidth', **(*c*)** Scenario 3 'Reduced cost service', **(*d*)** Scenario 4 'Locally congested connection'

EES, whereas for the scenario with battery storage the cost is 73.57 €, achieving a 10.47% of cost saving in total.

5.2.2 Impact of network emulation on EMS performance: The performance of the EMS is affected by the emulation of different network conditions. In comparison with the reference scenario 1, the difference in the operation costs for scenario 2 is 3.5%, for scenario 3 the deviation is 2.0%, and for scenario 4 the mismatch is 5.0%. Following this, it can be noted that the service with less restricted network conditions as emulated with scenario 3 affects the optimal solution the least. Larger latency and package losses seem to cause the most impact, as experienced with the locally congested connection of scenario 4. It affects the branch and bound algorithm and prevents it from achieving the optimal solution in several time steps. The highly reduced throughput of scenario 2, as shown in Fig. 8*b*, causes a noticeable effect. However, the influence is less pronounced as for scenario 4. For all scenarios, the solver is able to find a feasible solution within an optimality gap of 5%.

To further illustrate the impact of the different network conditions, the resulting sequences of power exchange with the grid for one building are compared in Fig. 10. The graph of scenario 3 closely follows the one of reference scenario 1, whereas the additional bandwidth boundaries of scenario 2 cause a larger deviation with a less optimal operation. The graph for scenario 4 is very similar to the one of scenario 2 and is not shown.

6 Conclusion

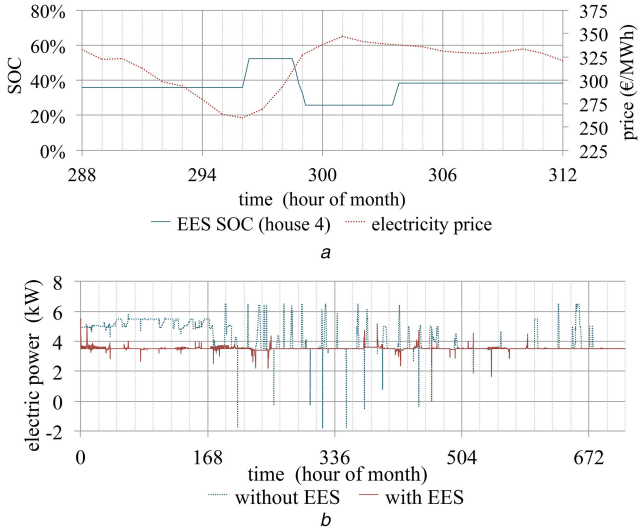

Fig. 9 *Use-case control performance*
(*a*) Electricity price profile for Stockholm area and battery SOC over time for building #4, 13th day of the month, **(*b*)** Power exchange with distribution grid over time for building #4, one month

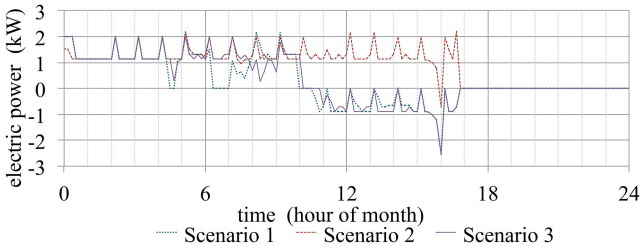

Fig. 10 *Power exchange with distribution grid over time for building #1, on first day*

A VSGL for co-simulation and evaluation of the smart grid was developed and implemented, integrating laboratory resources located in Berlin, Helsinki, and Stockholm. In particular, the proposed communication platform supports the testing of communication and control functions for distributed resources, offering access to diverse hardware equipment and software tools of geographically spread laboratories. Based on measurements of latency, throughput, and robustness of the communication involved, the developed platform was shown to be of practical value in the co-simulation of EMSs. The flexibility to draw from resources of diverse laboratories in real time is a valuable asset. The benefits of combining expertise and resources of distributed laboratory sites by using modern information and communication technologies have become evident.

While in this work the VSGL was used to validate the performance of EMSs under various communication network conditions, in the future the range of the virtual laboratory will also be used to study the effect of communication service breakdowns and their impact. As such, the VSGL will give further important insight on efficiency and robustness of the smart grid.

7 Acknowledgments

The authors acknowledge the support of the European Institute of Innovation and Technology (EIT) enabling this research and the development of the Virtual Smart Grid Laboratory.

8 References

[1] Perkonigg, F., Brujic, D., Ristic, M.: 'Platform for multiagent application development incorporating accurate communications modeling', *IEEE Trans. Ind. Inf.*, 2015, **11**, (3), pp. 728–736

[2] Yan, Y., Qian, Y., Sharif, H., *et al.*: 'A survey on smart grid communication infrastructures: motivations, requirements and challenges', *IEEE Commun. Surv. Tutor.*, 2013, **15**, (1), pp. 5–20

[3] Cao, Y., Jiang, T., He, M., *et al.*: 'Device-to-device communications for energy management: A smart grid case', *IEEE J. Sel. Areas Commun.*, 2016, **34**, (1), pp. 190–201
[4] Budka, K.C., Deshpande, J.G., Doumi, T.L., *et al.*: 'Communication network architecture and design principles for smart grids', *Bell Labs Tech. J.*, 2010, **15**, (2), pp. 205–227
[5] Ma, R., Chen, H.-H., Huang, Y.-R., *et al.*: 'Smart grid communication: its challenges and opportunities', *IEEE Trans. Smart Grid*, 2005, **4**, (1), pp. 36–46
[6] Ciontea, C.-I., Pedersen, R., Le Fevre Kristensen, T., *et al.*: 'Smart grid control and communication: The SmartC2net Real-Time HIL approach'. IEEE PowerTech Eindhoven, July 2015, pp. 1–6
[7] Unsal, D.B., Koc, A.H., Yalcinoz, T., *et al.*: 'Medium voltage and low voltage applications of new power line communication model for smart grids'. IEEE Int. Energy Conf. (ENERGYCON), April 2016, pp. 116–120
[8] Papadopoulos, T.A., Kaloudas, C.G., Chrysochos, A.I., *et al.*: 'Application of narrowband power-line communication in medium-voltage smart distribution grids', *IEEE Trans. Power Deliv.*, 2013, **28**, (2), pp. 981–988
[9] Cecati, C., Hancke, G., Palensky, P., *et al.*: 'Guest editorial special section on information technologies in smart grids', *IEEE Trans. Ind. Inf.*, 2013, **9**, (3), pp. 1380–1383
[10] Wang, H., Qian, Y., Sharif, H.: 'Multimedia communications over cognitive radio networks for smart grid applications', *IEEE Wirel. Commun.*, 2013, **20**, (4), pp. 125–132
[11] Huang, J., Wang, H., Qian, Y., *et al.*: 'Priority-based traffic scheduling and utility optimization for cognitive radio communication infrastructure-based smart grid', *IEEE Trans. Smart Grid*, 2013, **4**, (1), pp. 78–86
[12] Ho, Q.-D., Gao, Y., Le-Ngoc, T.: 'Challenges and research opportunities in wireless communication networks for smart grid', *IEEE Wirel. Commun.*, 2013, **20**, (3), pp. 89–95
[13] Faruque, M.O., Dinavahi, V., Steurer, M., *et al.*: 'Interfacing issues in multi-domain simulation tools', *IEEE Trans. Power Deliv.*, 2012, **27**, (1), pp. 439–448
[14] Wang, B., Sechilariu, M., Locment, F.: 'Intelligent DC microgrid with smart grid communications: control strategy consideration and design', *IEEE Trans. Smart Grid*, 2012, **3**, (4), pp. 2148–2156
[15] Strunz, K., Abbasi, E., Huu, D.: 'DC microgrid for wind and solar power integration', *IEEE J. Emerging Sel. Top. Power Electron.*, 2014, **2**, (1), pp. 115–126
[16] Sechilariu, M., Wang, B., Locment, F.: 'Building integrated photovoltaic system with energy storage and smart grid communication', *IEEE Trans. Ind. Electron.*, 2013, **60**, (4), pp. 1607–1618
[17] Xu, L., Huang, D., Tsai, W.-T., *et al.*: 'Cloud-based virtual laboratory for network security education', *IEEE Trans. Educ.*, 2014, **57**, (3), pp. 145–150
[18] Belazreg, M., Halbaoui, K., Boulheouchat, M., *et al.*: 'Modelling, simulation and control of hybrid system integrating logic, dynamics, and constraints using hybrid automaton, APROS and mixed integer quadratic optimization algorithm'. 8th Int. Conf. on Modelling, Identification and Control (ICMIC), 2016, pp. 634–642
[19] Grüner, S., Frommer, J., Palm, F.: 'RESTful industrial communication with OPC UA', *IEEE Trans. Ind. Inf.*, 2016, **12**, (5), pp. 1832–1841
[20] Jurgelionis, A., Laulajainen, J.-P., Hirvonen, M., *et al.*: 'An empirical study of NetEm network emulation Functionalities'. Proc. of 20th Int. Conf. on Computer Communications and Networks (ICCCN), 2011, pp. 1–6
[21] Strunz, K., Wiezorek, C.: 'Development of the European virtual smart grid laboratory', *Ercim News Spec. Smart Energy Syst.*, 2013, **92**, pp. 10–11
[22] Parisio, A., Wiezorek, C., Kyntäjä, T., *et al.*: 'An MPC-based energy management system for multiple residential microgrids'. IEEE Int. Conf. on Automation Science and Engineering (CASE), August 2015, pp. 7–14
[23] Paridari, K., Parisio, A., Sandberg, H., *et al.*: 'Robust scheduling of smart appliances in active apartments with user behavior uncertainty', *IEEE Trans. Autom. Sci. Eng.*, IEEE CASE 2014 Special Issue, 2016, **13**, pp. 247–259
[24] 'DIN 5034 - Daylight in interiors': 'Standardization Committee Lighting Engineering (FNL) of the German Institute for Standardization (DIN)', 2011
[25] Sauer, K., Roessler, T., Hansen, C.: 'Modeling the irradiance and temperature dependence of photovoltaic modules in PVsyst', *IEEE J. Photovoltaics*, 2015, **5**, (1), pp. 152–158
[26] 'Photovoltaic Geographical Information System (PVGIS)': Institute for Energy and Transport (IET) of the European Commission. Available at http://re.jrc.ec.europa.eu/pvgis/, accessed 2 March 2016
[27] Miara, M.: 'Wärmepumpen: Heizen - Kühlen - Umweltenergie nutzen', in (Eds): '*BINE reference book*' (Fraunhofer IRB Verlag, Karlsruhe, 2013)
[28] 'CPLEX optimization subroutine library guide and reference, version 12.0' (CPLEX Division, ILOG Inc., Sunnyvale, CA, USA, 2012)
[29] 'DIN EN 15251:2007 - Indoor environmental input parameters for design and assessment of energy performance of buildings addressing indoor air quality, thermal environment, lighting and acoustics', Standardization Committee Heating, Ventilation and Air-conditioning (NHRS) of the German Institute for Standardization (DIN), 2007
[30] Stoll, P., Bag, G., Rossebø, J.: 'Scheduling residential electric loads for green house gas reductions'. 2nd IEEE PES Int. Conf. and Exhibition on Innovative Smart Grid Technologies, 2011, pp. 1–8